



HAL
open science

Introduction of Fragility Surfaces for a More Accurate Modeling of the Seismic Vulnerability of Reinforced Concrete Structures

Pierre Gehl, Darius Seyedi, John Douglas, Mahmoud Khiar

► **To cite this version:**

Pierre Gehl, Darius Seyedi, John Douglas, Mahmoud Khiar. Introduction of Fragility Surfaces for a More Accurate Modeling of the Seismic Vulnerability of Reinforced Concrete Structures. COMPDYN 2009 - ECCOMAS Thematic Conference on Computational Methods in Structural Dynamics and Earthquake Engineering, Jun 2009, Rhodes, Greece. Paper n°228. hal-00560523

HAL Id: hal-00560523

<https://brgm.hal.science/hal-00560523>

Submitted on 28 Jan 2011

HAL is a multi-disciplinary open access archive for the deposit and dissemination of scientific research documents, whether they are published or not. The documents may come from teaching and research institutions in France or abroad, or from public or private research centers.

L'archive ouverte pluridisciplinaire **HAL**, est destinée au dépôt et à la diffusion de documents scientifiques de niveau recherche, publiés ou non, émanant des établissements d'enseignement et de recherche français ou étrangers, des laboratoires publics ou privés.

INTRODUCTION OF FRAGILITY SURFACES FOR A MORE ACCURATE MODELING OF THE SEISMIC VULNERABILITY OF REINFORCED CONCRETE STRUCTURES

Pierre Gehl¹, Dariush Seyedi¹, John Douglas¹ and Mahmoud Khier¹

¹BRGM - ARN
3, avenue Claude Guillemin
BP 36009 - 45060 ORLEANS Cedex 2
e-mail: p.gehl@brgm.fr

Keywords: Reinforced concrete building, fragility curve, fragility surface, non-linear time-history analysis, vulnerability assessment, strong-motion parameters.

Abstract. *Earthquake shaking represents complex loading to a structure. It cannot be accurately characterized by a single parameter such as peak ground acceleration. The goal of this work is to compare the role of various strong-motion parameters on the induced damage in the structure using numerical calculations. The most influential parameters are then used to build multi-variable fragility functions, in order to reduce some of the uncertainty inherent in the response to seismic loading.*

To this end, a robust structural model of an eight-story reinforced concrete building on which dynamic calculations can be performed at an acceptable cost is used. In the model, all elements have a linear behaviour, except the ends of each column and each beam to which a nonlinear behaviour based on damage mechanics and plasticity type (plastic-hinges model) is assigned [1]. Several hundred nonlinear dynamic analyses are carried out on the structure and the damage levels are identified using the inter-story drift ratio, which can be linked to standard damage scales.

The spectral displacements, SD s, at the first two modal periods T_1 and T_2 are used to represent the seismic loading as the most useful parameters reflecting the structure's response [1]. Each pair of points $[SD(T_1), SD(T_2)]$ is associated with a probability of exceeding a given damage level. This probability P is evaluated by considering the damage levels attained by other points located in its neighbourhood. A scalar parameter $R = f[SD(T_1), SD(T_2)]$ is then built up and we can construct an analytic equation for the fragility curve $P = g(R) = g(f[SD(T_1), SD(T_2)])$.

This results in an equation for a fragility surface that offers a more complete and accurate view of the structure's vulnerability. A comparison between different profiles obtained by the generated fragility surfaces and conventional fragility curves shows the significant role of the second parameter in accurately estimating the probability of damage.

Such fragility surfaces can be implemented within earthquake risk evaluation tools and they should provide more precise damage estimations. It is expected that this procedure can lead to more accurate land-planning and retrofitting policies for risk mitigation.

1 INTRODUCTION

A variety of vulnerability analysis procedures have been followed in the past, ranging from the analysis of equivalent single-degree-of-freedom systems [3], adaptive pushover analysis of multistory models [2] to nonlinear time-history analyses of 3D models of RC structures [4]. The choices made for the analysis method, structural idealization, seismic hazard characterization and damage models strongly influence the derived curves and have been seen to cause significant discrepancies in seismic risk assessments made by different groups for the same location, structure type and seismicity [5].

The classical procedures are based on the study of simplified substitute structures that are not capable of accounting for the load redistribution inside structures due to local nonlinearities. The objective of damage assessment is to evaluate expected losses based on sufficiently detailed analyses and the evaluation of the vulnerability characteristics at a given level of earthquake ground motions. The conditional probability that a particular building will reach a certain damage state should be determined using a fragility model. It consists of a suite of fragility functions defining the conditional probability of reaching or exceeding a certain damage state.

Earthquake shaking applies complex loading to a structure, which cannot be accurately characterized by a single parameter (e.g. peak ground acceleration, *PGA*, or macroseismic intensity). However, in current vulnerability assessment methods, fragility curves are often developed by using a single parameter to relate the level of shaking to the expected damage. This standard method to develop fragility curves neglects the variability in the estimated damage caused by the use of a single ground-motion parameter, which means that this uncertainty cannot properly be propagated to subsequent parts of the risk analysis nor can the importance of this variability be assessed.

The main objective of the ANR-funded VEDA (Seismic vulnerability of structures: A damage mechanics approach) project is to improve the existing methods of vulnerability evaluation by introducing the fragility surface concept for current reinforced concrete structures. In this approach, the shaking is characterized by two intensity measure (IM) parameters. The selected IM parameters should ideally be poorly correlated for efficient characterization of the shaking. On the contrary, the structural damage must be correlated to the selected parameters. It is expected that an increase from one to two IM parameters will lead to a significant reduction in the scatter in the fragility curve, which when using more than one parameter is a surface.

The damage level of a typical reinforced concrete structure is evaluated by the use of nonlinear numerical calculations. By considering the parts of the structure that would suffer significant damage during strong ground motions (plastic hinges), an adequate 3D nonlinear robust-yet-simplified finite element model is created to allow numerous computations. The maximum inter-story drift ratio is used to define the damage level of the studied structure. Such a study can help find a small number of ground-motion parameters that lead to, when used together to characterize the shaking, the smallest scatter in the estimated damage. Fragility surfaces are then proposed for the studied structure.

2 MODEL DEFINITION AND DAMAGE ANALYSIS

2.1 Structural model

The main goal of vulnerability assessment methods is to estimate the seismic response of existing buildings. For this purpose we have used a structural model described in Seyedi et al. [1]. This is an eight-storey regular frame reinforced concrete (RC) structure. The structural system of the building mainly consists of parallel shear walls in the *Y* direction, and an RC

beam-columns frame in the X direction.

In the framework of the VEDA project, this building was meshed by NECS, using shells to represent slabs and walls, and linear beam elements for beams and columns. The damaging process is modelled thanks to plastic hinges located at the extremities of each beam and column [1].

The earthquake is applied to the structure in the X direction as an acceleration time-history. Only one horizontal component was used for each analysis. Calculations were carried out with Code Aster [6] finite element program, using the Newton-Raphson implicit algorithm.

2.2 Nonlinear time-history analysis

In this paper it is assumed that the analyzed structure is located in the French Antilles (Guadeloupe and Martinique), which is a region affected by both crustal and subduction (interface: shallow-dipping thrust events and intraslab: deep, generally normal-faulting, events) earthquakes. Therefore, a set of strong-motion records were compiled that is consistent with the seismicity of this region. A magnitude-distance-earthquake-type filter is applied to a large database of strong-motion records from various regions of the world (mainly the Mediterranean region, the Middle East, western North America, central America, Japan and Taiwan) to exclude records from magnitudes and distances that are not possible for the French Antilles. Also records from small earthquakes and great distances were excluded since such weak motions will not lead to significant damage for the structure analyzed here.

This led to a selection of 169 natural accelerograms that could potentially be used as input to the structural modelling to construct the fragility surfaces. However, since the whole range of possible motions is not covered by the selected accelerograms it was decided to augment the input time-history dataset with records simulated using the non-stationary stochastic method of Pousse et al. [7], which is an extension of the procedure of Sabetta and Pugliese [8]. This resulted in the generation of 571 exploitable synthetic accelerograms.

In total, we used 740 strong-motion records (571 synthetic ones and 169 natural ones) as input to time-history analyses. An extra advantage of using these simulated ground motions over the natural accelerograms is that the structural modeling was faster due to the generally shorter length of the records.

2.3 Results

As explained in previous section, 740 non-linear time-history analyses were performed on the structural model and, for each simulation, the highest inter-storey drift ratio (ISDR) was extracted as the structure response to the seismic input.

An advantage of using the ISDR to evaluate the damage level of a building is that this variable is fairly intuitive and was widely used in previous studies. Based on thousands of observations Rossetto and Elnashai [9] developed empirical functions that correlate the ISDR and the damage level for different types of European RC buildings. Depending on the type of RC structure, relationships between the ISDR and an homogenized reinforced concrete damage index (DI_{HRC}) are proposed. Given the model of the studied structure, it was decided to use the relation for non-ductile moment-resisting frames to estimate the damage index of the structure (see Equation 1), this relationship also has the advantage of presenting a satisfactory correlation coefficient ($R^2 = 0.991$):

$$DI_{HRC} = 34.89 \ln(ISDR) + 39.39 \quad (1)$$

DI_{HRC} can then be converted to the EMS-98 damage scale [10]: the correlation between DI_{HRC} and EMS-98 damage level is shown in Table 1.

DI_{HRC} value	EMS-98 damage level
$DI_{\text{HRC}} < 0$	D0
$0 \leq DI_{\text{HRC}} < 30$	D1
$30 \leq DI_{\text{HRC}} < 50$	D2
$50 \leq DI_{\text{HRC}} < 70$	D3
$70 \leq DI_{\text{HRC}} < 100$	D4
$100 \leq DI_{\text{HRC}}$	D5

Table 1: Correlation between the damage index DI_{HRC} and the EMS-98 damage level [9].

With the ISDR values obtained from the 740 simulations, the objective is now to find two ground-motion parameters that have the most influence on the building’s response, in order to build fragility surfaces. Orthogonal parameters are sought that characterize different aspects of the shaking, e.g. the amplitude, frequency content and duration, so that the fewest number of parameters is needed. Problems associated with the choice of parameters for ground motion and damage characterization can be identified in almost all existing vulnerability relationships [9]. The parameter chosen to represent ground motion in the construction of vulnerability curves must be both representative of the damage potential of earthquakes and easily quantifiable from knowledge of the earthquake characteristics.

In this study, we selected several strong-motion intensity parameters that can be well estimated through GMPEs and that are likely to have a strong influence on the building response. Table 2 presents the linear equations connecting the inter-storey drift ratio and the investigated strong-motion intensity parameters, x .

This study led to the choice of the spectral displacement as a useful variable for constructing the fragility surfaces (see Table 2). The choice of the periods at which the spectral displacement was examined was guided by eigenvalue analysis of the modeled building. The two main eigenperiods along the X direction (the direction where the seismic input is applied) were found to be 1.26 and 0.41s respectively and, hence, SD s at these two periods were chosen as the strong-motion IM parameters.

A quick look at the distribution of selected time-histories in $SD(1.26s)$ – $SD(0.41s)$ space (see Figure 1) reveals that the two selected parameters seem strongly correlated. Nevertheless these two parameters are sufficiently uncorrelated (correlation coefficient of 0.83) to be used to build a fragility surface, e.g. for a $SD(1.26s)$ of 0.01 m Figure 1 shows that $SD(0.41s)$ can range between roughly $6 \cdot 10^{-4}$ m and 0.02 m. Only some extreme situations (i.e. low $SD(1.26s)$ and very high $SD(0.41s)$ and vice versa) are not represented: these situations are not, in fact, realistic for earthquake shaking.

3 DEVELOPMENT OF FRAGILITY SURFACES

3.1 Conventional fragility curves

A first step, before tackling the issue of fragility surfaces, was to develop conventional fragility curves, based on only one IM parameter. Shinozuka et al. [11] [12] developed an analytical function that expresses the fragility curve in the form of a two-parameter lognormal distribution function (Equation 2).

Parameter	Description	Equation	Correlation coefficient R^2
$SD(1.26s)$	Spectral displacement at the period of the first mode	$5.6025x - 0.025$	0.837
$SD(0.41s)$	Spectral displacement at the period of the second mode	$20.99x - 0.0084$	0.650
PGA	Peak ground acceleration	$0.1239x + 0.0213$	0.578
AI	Arias intensity	$0.1506x + 0.1479$	0.565
AUD	Absolute uniform duration (based on a threshold of 0.03g)	$0.0834x + 0.0454$	0.532
RSD	Relative significant duration (based on the interval between 5 and 95% Arias intensity)	$-0.0025x + 0.3045$	0.305
RUD	Uniform relative duration (based on a threshold of 10% PGA)	$-0.0027x + 0.2972$	0.003
NC	Equivalent number of effective cycles (Rainflow method)	$0.0191x + 17.784$	0.000

Table 2: Correlation between various strong-motion parameters (x) and the building inter-story drift ratio (ISDR). Equation reported is derived through linear regression.

$$F(x) = \phi \left(\frac{\ln(x) - \ln(\alpha)}{\beta} \right) \quad (2)$$

where x represents the strong motion parameter (e.g. the spectral displacement), and F the standardized normal distribution function. The two parameters α and β represent the median and the lognormal standard deviation respectively and are computed so as to maximize the likelihood function [11] [12], given by Equation 3.

$$M = \prod_{k=0}^N [F(x_k)]^{y_k} [1 - F(x_k)]^{1-y_k} \quad (3)$$

where N is the total number of simulations, x_k the spectral displacement of the k -th accelerogram, and y_k is equal to 1 or 0, whether the structure has reached the given damage state or not (realization from a Bernoulli experiment). For both of the studied IM parameters ($SD(1.26s)$ and $SD(0.41s)$), we developed four fragility curves corresponding to the four damage levels for the studied structure. Figure 2 and Table 3 present the results for $SD(1.26s)$ as the single IM parameter.

3.2 Development of fragility surfaces using the ‘neighbourhood’ method

The following procedure has been developed to construct the fragility surfaces. For the two chosen strong-motion intensity parameters (here $SD(1.26s)$ and $SD(0.41s)$, being the first and second natural periods of the building), we build a x - y space containing 740 points of coordinates (x_i, y_i) , x and y representing the two IM parameters. This space is associated with the following norm, between points $A(x_1, y_1)$ and $B(x_2, y_2)$:

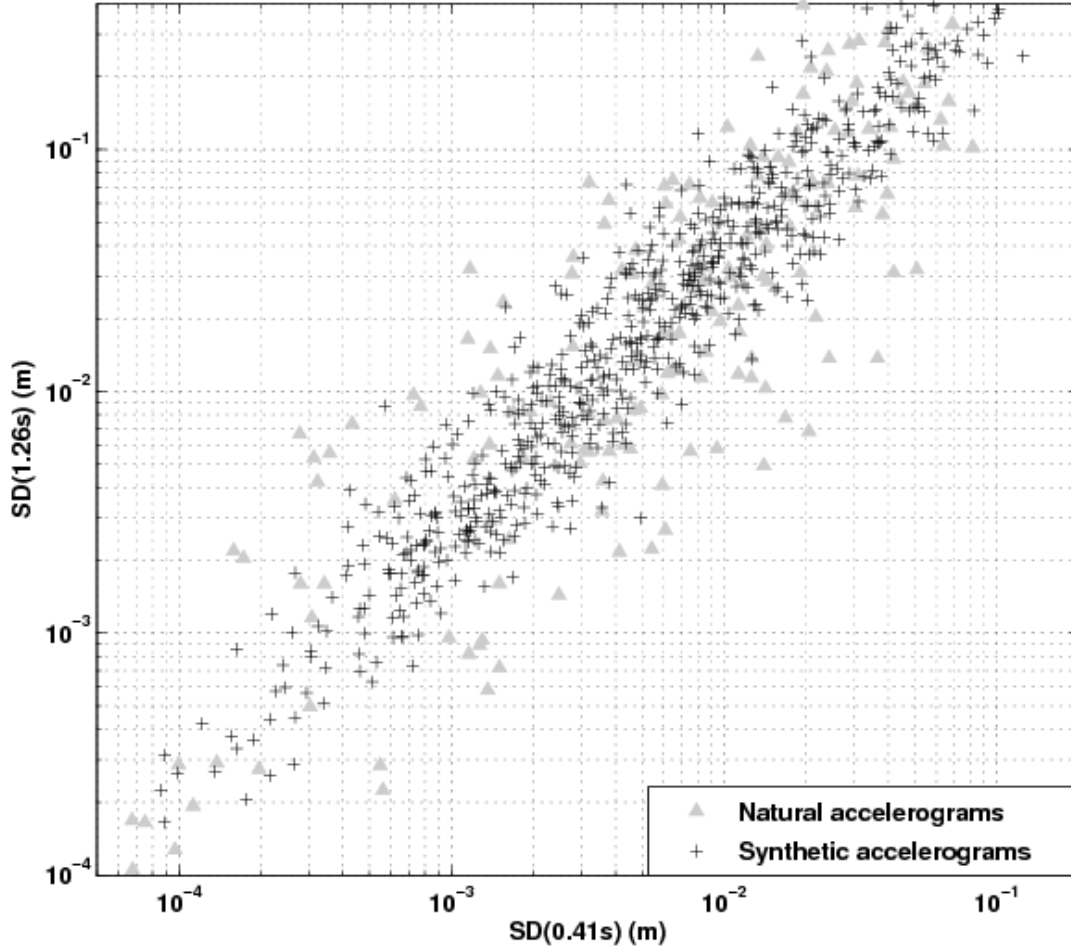


Figure 1: Distribution of selected time-histories in $SD(1.26s)$ – $SD(0.41s)$ space. The crosses (and the grey triangles) represent the synthetic (and the real) accelerograms respectively.

$$d(A, B) = \sqrt{\left[\frac{\ln(\frac{x_1}{x_2})}{\ln(\frac{x_{max}}{x_{min}})} \right]^2 + \left[\frac{\ln(\frac{y_1}{y_2})}{\ln(\frac{y_{max}}{y_{min}})} \right]^2} \quad (4)$$

It was chosen to introduce a logarithm scale because the use of a conventional Euclidian norm was not adapted to the range of values (several powers of ten) spanned by $SD(1.26s)$ and $SD(0.41s)$. To avoid bias due to differently-scaled parameters this norm was also normalized by the amplitude ($x_{max} - x_{min}$) of each parameter.

For each of the 740 points we defined a neighbourhood V of radius d , where we can evaluate the probability to reach or exceed the damage state D_k :

$$P(D > D_k) = \frac{N_{V,k}}{N_{V,tot}} \quad (5)$$

In Equation 5, $N_{V,tot}$ is the total population in the neighbourhood V and $N_{V,k}$ denotes the number of points for which the damage state reaches or exceeds D_k . However, not all the points

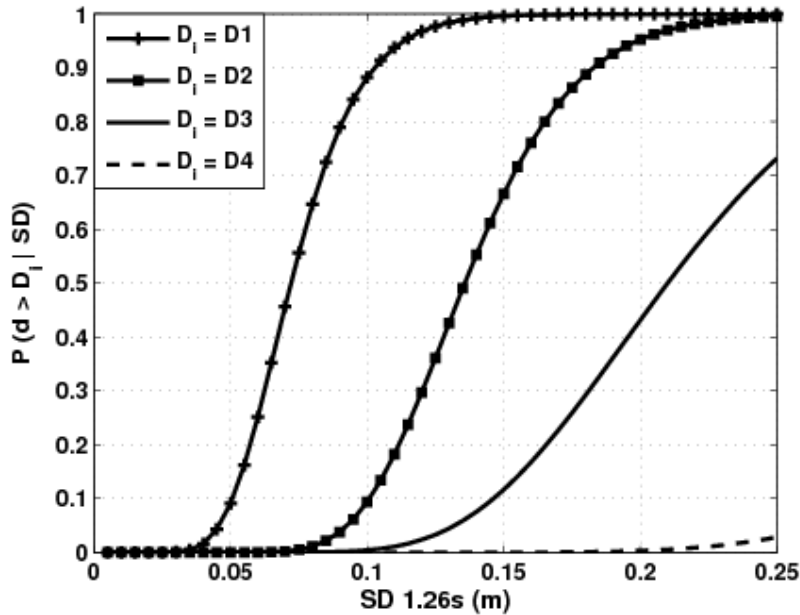


Figure 2: Fragility curves developed by Shinozuka et al's method, with $SD(1.26s)$ as the IM parameter.

	D1	D2	D3	D4
α	0.0721	0.1358	0.2100	0.4206
β	0.2753	0.2320	0.2822	0.2732

Table 3: Parameters of the equation for each fragility curve, with $SD(1.26s)$ as the IM parameter.

have sufficient points close enough to produce an accurate surface. Hence, it was decided to consider only nodes whose neighbourhood contains at least five points. This approach enabled us to evaluate the probability for each of the 740 points in the $SD(1.26s)$ – $SD(0.41s)$ space.

However, surfaces generated using this original approach present some anomalies (such as local peaks). This observation stresses the main issue of this approach: in order to define the neighbourhood V of each point, a value of the radius d has to be chosen more or less arbitrarily.

Greater values of the radius d help to smooth the surface, but there is a risk of generating a too blurry description of the fragility (loss in precision). On the contrary, to obtain a sharper image of the structures vulnerability, it is recommended to decrease the value of d (at the expense of regularity). After a small sensitivity study, it was chosen here to set $d = 0.1$.

Another drawback of this method is the unreliability of the results at the edges of the dataset: this unreliability should be taken into account when viewing fragility surfaces by recalling that the region of validity of the surfaces lies within V with its point at the origin. As a result, in the scope of both computational stability and accuracy, an optimisation of the method used to calculate surfaces remains a key goal if fragility surfaces are to become a viable alternative to fragility curves.

3.3 Analytical definition of fragility surfaces

This section presents an attempt at proposing an analytical definition for the fragility surfaces, taking the method described in previous section a step further.

The 740 probability values for reaching or exceeding damage state $D1$, evaluated in the previous section, were plotted on a 2D-graph, as a function of one parameter only ($SD(1.26s)$ or $SD(0.41s)$). The two plots are presented in Figure 3: as expected, the graphs show great scatter, proving once again the need for a second parameter to give a better description of the structure vulnerability.

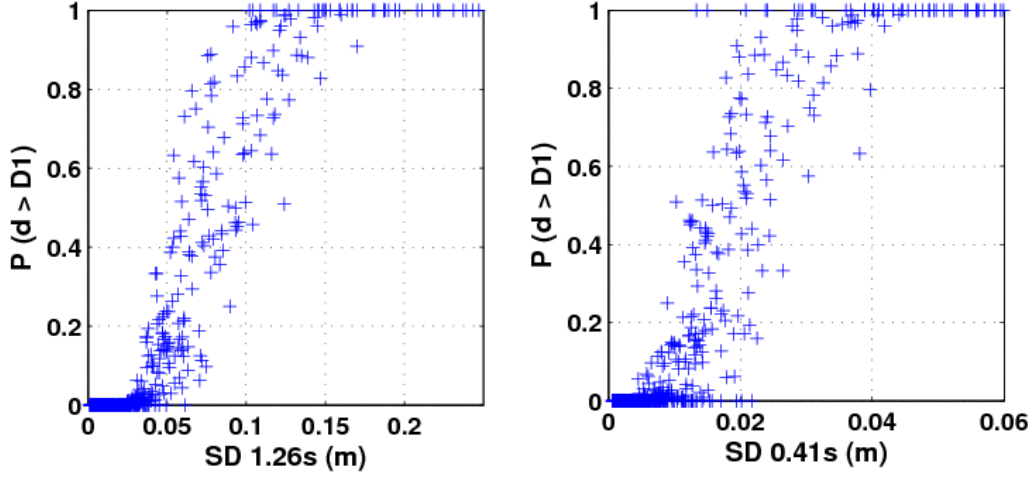


Figure 3: Fragility curves for the damage level $D1$, based on parameters $SD(1.26s)$ and $SD(0.41s)$, generated with the points used for the development of fragility surfaces presented in previous section.

An analysis of the fragility surfaces presented previously made us think that a hybrid parameter (such as the logarithmic distance between a point A of the $SD(1.26s)$ – $SD(0.41s)$ space and the origin (10^{-4} , 10^{-4})) could be a good candidate for building vector-based fragility curves:

$$R[SD(1.26s), SD(0.41s)] = \sqrt{\ln^2\left(\frac{SD(1.26s)}{10^{-4}}\right) + \ln^2\left(\frac{SD(0.41s)}{10^{-4}}\right)} \quad (6)$$

Each of the 740 points are associated with this new variable R , and the probability of reaching or exceeding damage state $D1$ with R on the abscissa is plotted (see Figure 4).

Figure 4 clearly shows the reduction in the scatter of the probability data: the plotted points directly take the shape of a normal distribution cumulative function. It is then possible to fit the points by an analytical function, depending on the variable R (hence it is a function of the two variables $SD(1.26s)$ and $SD(0.41s)$), and defined by Equation 7:

$$P_k(d > D_k | R) = 0.5 \left[1 + \operatorname{erf} \left(\frac{\ln(R) - \ln(\alpha_k)}{\beta_k \sqrt{2}} \right) \right] \quad (7)$$

The same procedure is applied to damage states $D2$, $D3$ and $D4$, and Table 4 sums up the parameters of Equation 7, for all damage states.

Thanks to Equation 7, we now have the equation of a surface, linking the probability to the two desired parameters $SD(1.26s)$ and $SD(0.41s)$. The four analytical fragility surfaces for all damage states are displayed in Figure 5.

The analytical expression enables users of fragility surfaces to properly exploit the vulnerability data (the input of $SD(1.26s)$ and $SD(0.41s)$ parameters returns a calculated probability value).

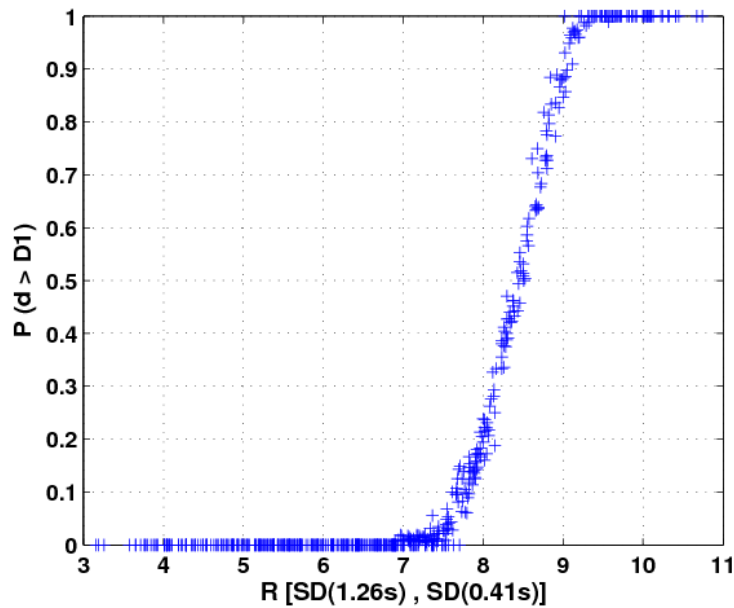


Figure 4: Fragility curve for the damage level $D1$, based on parameter R , generated with the points used for the development of fragility surfaces presented in previous section.

	D1	D2	D3	D4
α	8.4197	9.3066	9.8339	11.4569
β	0.0587	0.0591	0.0635	0.1026

Table 4: Parameters of the equation for each fragility curve, with $R[SD(1.26s), SD(0.41s)]$ as the IM parameter.

4 CONCLUSIONS

The most widely-applied methods used to model the seismic vulnerability of structures (i.e. through fragility curves) often represent the ground motion by a single parameter (e.g. PGA). However, a single parameter cannot fully represent the effect of an earthquake on the seismic response of the structure. It is expected that an increase from one to two ground-motion parameters would lead to a significant reduction in the scatter in the fragility curve, which when more than one parameter is used will be a surface.

To this end, a nonlinear structural model to calculate the induced damage in a reinforced concrete structure has been developed within the framework of the VEDA project. Several hundreds of natural and synthetic accelerograms have been used, and a strong correlation between SD at the first two eigenperiods (T_1 and T_2) and the maximum inter-story drift ratio (as the damage measure) is observed.

Based on the obtained results, fragility surfaces that relate the strong-motion intensity (represented by the two parameters) to the possible damage of the structure are developed. A comparison between different profiles obtained by the obtained fragility surfaces and conventional fragility curves shows the significant role of the second parameter in calculated damage probability. If only one parameter, e.g. $SD(T_1)$, is considered, we can build a mean curve that does not incorporate the variability due to the other characteristics of the ground motions.

Because of a lack of field data some of the properties used in our simulations have been

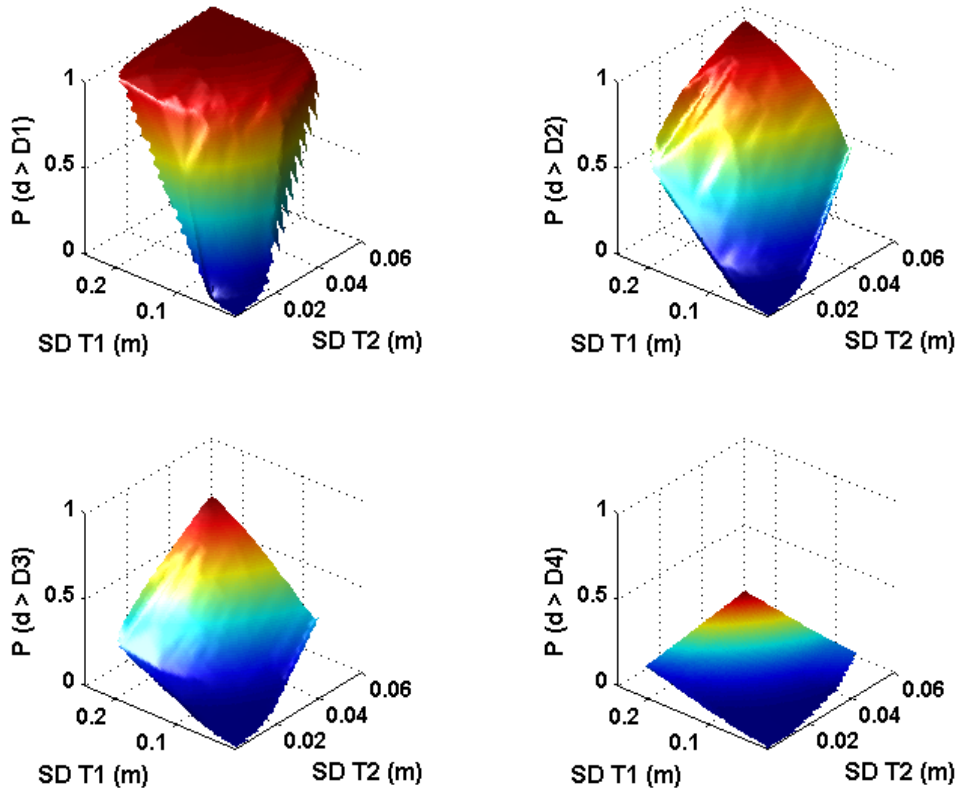


Figure 5: Fragility surfaces for the four damage states, derived from the analytical Equation 7, and based on $SD(1.26s)$ and $SD(0.41s)$.

estimated. Therefore, results of this study should be only considered qualitatively since the quantitative results are sensitive to the assumed material properties and construction details. In the future, a more detailed damage analysis should be performed in order to properly evaluate the role of all parameters. In this view, the effect of each parameter on several damage indicators (e.g. energy based indicators and combination measures) can be investigated. The strong-motion parameters must be chosen individually for each structural type so as to incorporate the dynamic response of the structure.

5 ACKNOWLEDGEMENTS

The work presented in this article has been supported by French Research National Agency (ANR) through CATTEL-2005 program (project Seismic vulnerability of structures: A damage mechanics approach (VEDA) under grant number ANR – 05 – CATT – 017). We thank the providers of the strong-motion and the structural data used. The authors wish also to thank their colleagues in the VEDA project (Dr. Shahrokh Ghavamian, Dr. Nader Mezher and Dr. Luc Davenne) for providing the structural model and designing an accurate mesh of the building. In addition, we thank Dr Guillaume Pousse for sending us his computer program to simulate strong-motion records using his method. Finally, we thank Dr Tiziana Rossetto and Mr Mutahar Chalmers, whose comments led to significant improvements to this study.

REFERENCES

- [1] D. Seyedi, P. Gehl, J. Douglas, L. Davenne, N. Mezher, S. Ghavamian, *Development of seismic fragility surfaces for reinforced concrete buildings by means of nonlinear time-history analysis*. Earthquake Engineering and Structural Dynamics, under revision.
- [2] T. Rossetto, A. Elnashai, *A new analytical procedure for the derivation of displacement-based vulnerability curves for populations of RC structures*. Engineering Structures, **27**, 397–409, 2005.
- [3] K. Mosalam, G. Ayala, R. White, C. Roth, *Seismic fragility of LRC frames with and without masonry infill walls*. Journal of Earthquake Engineering, **1**, 683–719, 1997.
- [4] A. Singhal, A. Kiremidjian, *A method for earthquake motion damage relationships with application to reinforced concrete frames*. Research Report NCEER-97-0008 State University of New York at Buffalo: National Center for Earthquake Engineering, 1997.
- [5] M. Priestley, *Displacement-based approaches to rational limit states design of new structures*. 11th European Conference on Earthquake Engineering, Rotterdam, AA Balkema, 1998.
- [6] Code Aster, *Code d'Analyses des Structures et Thermomécanique pour Etudes et Recherches*. www.code-aster.org EDF R&D, 2008.
- [7] G. Pousse, L.F. Bonilla, F. Cotton, L. Margerin, *Non stationary stochastic simulation of strong ground motion time histories including natural variability: Application to the K-net Japanese database*. Bulletin of Seismological Society of America, **96**(6), 2103–2117, 2006.
- [8] F. Sabetta, A. Pugliese, *Estimation of response spectra and simulation of nonstationary earthquake ground motions*. Bulletin of Seismological Society of America, **86**(2), 337–352, 1996.
- [9] T. Rossetto, A. Elnashai, *Derivation of vulnerability functions for European-type RC structures based on observational data*. Engineering Structures, **25**, 1241–1263, 2003.
- [10] European Council, *European Macroseismic Scale 1998 (EMS-98)*. Cahier du Centre Européen de Géodynamique et de Sismologie, G. Grnthal (Eds.), **15**, 1998.
- [11] M. Shinozuka, *Statistical analysis of bridge fragility curves*. US - Italy Workshop on Protective Systems for Bridges, New-York, April 26-28, 1998.
- [12] M. Shinozuka, Q. Feng, J. Lee, T. Naganuma, *Statistical analysis of fragility curves*. Journal of Engineering Mechanics, ASCE, **126**(12), 1224–1231, 2000.